

Article

Rapid Detection of Cd²⁺ Ions in the Aqueous Medium Using a Highly Sensitive and Selective Turn-On Fluorescent Chemosensor

Maria Sadia ¹, Jehangir Khan ¹, Rizwan Khan ², Abdul Waheed Kamran ¹, Muhammad Zahoor ^{3,*} , Riaz Ullah ⁴, Ahmed Bari ⁵  and Essam A. Ali ⁵ 

¹ Department of Chemistry, University of Malakand, Chakdara 18800, Pakistan

² Department of Electrical Engineering, Kwangwoon University Seoul, Seoul 01897, Republic of Korea

³ Department of Biochemistry, University of Malakand, Chakdara 18800, Pakistan

⁴ Department of Pharmacognosy, College of Pharmacy, King Saud University, Riyadh 11495, Saudi Arabia

⁵ Department of Pharmaceutical Chemistry, College of Pharmacy, King Saud University, Riyadh 11495, Saudi Arabia

* Correspondence: mohammadzahoorus@yahoo.com

Abstract: Herein, a novel optical chemosensor, (**CM1** = 2, 6-di((E)-benzylidene)-4-methylcyclohexan-1-one), was designed/synthesized and characterized by ¹H-NMR and FT-IR spectroscopy. The experimental observations indicated that **CM1** is an efficient and selective chemosensor towards Cd²⁺, even in the presence of other metal ions, such as Mn²⁺, Cu²⁺, Co²⁺, Ce³⁺, K⁺, Hg²⁺, and Zn²⁺ in the aqueous medium. The newly synthesized chemosensor, **CM1**, showed a significant change in the fluorescence emission spectrum upon coordination with Cd²⁺. The formation of the Cd²⁺ complex with **CM1** was confirmed from the fluorometric response. The 1:2 combination of Cd²⁺ with **CM1** was found optimum for the desired optical properties, which was confirmed through fluorescent titration, Job's plot, and DFT calculation. Moreover, **CM1** showed high sensitivity towards Cd²⁺ with a very low detection limit (19.25 nM). Additionally, the **CM1** was recovered and recycled by the addition of EDTA solution that combines with Cd²⁺ ion and, hence, frees up the chemosensor.

Keywords: chemosensor; curcumin; heavy metals; aqueous medium; high sensitivity



Citation: Sadia, M.; Khan, J.; Khan, R.; Kamran, A.W.; Zahoor, M.; Ullah, R.; Bari, A.; Ali, E.A. Rapid Detection of Cd²⁺ Ions in the Aqueous Medium Using a Highly Sensitive and Selective Turn-On Fluorescent Chemosensor. *Molecules* **2023**, *28*, 3635. <https://doi.org/10.3390/molecules28083635>

Academic Editor: Barbara Panunzi

Received: 23 February 2023

Revised: 19 April 2023

Accepted: 20 April 2023

Published: 21 April 2023



Copyright: © 2023 by the authors. Licensee MDPI, Basel, Switzerland. This article is an open access article distributed under the terms and conditions of the Creative Commons Attribution (CC BY) license (<https://creativecommons.org/licenses/by/4.0/>).

1. Introduction

Cadmium (Cd²⁺) is one of the most hazardous and carcinogenic heavy metals, and it is widely employed in various industrial applications, such as the fabrication of metal alloys, batteries, electroplating films, and nuclear reactor control rods [1]. The effect of Cd²⁺ pollution should not be underestimated [2]. As a heavy metal ion with a biological half-life of 20 to 30 years, Cd²⁺ accumulates in the human body through contaminated water, air, soil, or other sources, leading to a variety of disorders of the kidney, liver, heart, lung, or other organs. Even if the accumulated Cd²⁺ content in the body is very low, it can still result in several health problems, including potentially fatal diseases, such as diabetes, cancer, and chondropathy [3]. Currently, there are several efficient methods to detect Cd²⁺: atomic absorption spectrometry (AAS) [4], inductively coupled plasma mass spectrometry (ICP-MS) [5], atomic fluorescence spectrophotometry (AFS) [6], the electrochemical method [7,8], and the fluorescence probe method [9–11]. Compared to the fluorescent probe technique, AAS, AFS, and ICP-MS need complex and expensive instruments, complicated sample preparation, and the electrochemical method, which has the disadvantage of poor selectivity.

The main advantage of the fluorescent probe technique is its high sensitivity, visibility, and rapid response. In addition, simple operation, low cost, and a wide linear range for heavy metal ions are also clear advantages. Therefore, the development of highly selective colorimetric/fluorescent chemosensors for the detection of harmful metal ions

from environmental samples has received considerable interest due to their high sensitivity, selectivity, quick detection time, and cost-effectiveness [12–14]. In recent years, a large number of fluorescent probes with diverse scaffolds, such as quinoline, rhodamine, pyrene, boron-dipyrromethene (BODIPY), and anthraquinone, etc. have been developed with sensitivity, selectivity, and real-time detection of Cd^{2+} [12,15–20,20]. However, only a few examples of chemosensors have been reported where a considerable fluorescence enhancement is observed upon Cd^{2+} ion binding in aqueous medium [21–23]. The major difficulty in detecting Cd^{2+} is due to the relatively similar binding characteristics of Cd^{2+} with Zn^{2+} and Hg^{2+} cations, as they are in the same periodic table group. It is challenging to develop a probe for Cd^{2+} that does not exhibit the interference of Zn^{2+} and Hg^{2+} cations. Although a large number of fluorescent sensors have already been reported with success to differentiate Cd^{2+} from Zn^{2+} and Hg^{2+} cations, the majority of them have low water solubility with a lack of sensitivity and selectivity [24–28]. Therefore, designing and developing fluorescent probes with high water solubility and selectivity is a great challenge for the researcher. Herein, we report the design and synthesis of a water-soluble and simple fluorescent turn-on chemosensor comprising a **CM1** fluorophore, selectively detecting Cd^{2+} over other relevant metal ions in aqueous samples. Due to possessing the best coordination sites, it was capable of forming stable complexes with Cd^{2+} ions. The **CM1** showed a fast response, high sensitivity, and excellent selectivity for Cd^{2+} ion detection in an aqueous medium. The sensing mechanism of **CM1** was based on competitive binding with Cd^{2+} ions among different metal ions. Ethylenediaminetetraacetic acid (EDTA) was used as a chelating agent in reversibility studies.

2. Results and Discussion

2.1. Spectroscopic Studies

The UV-Vis absorption spectra were investigated, and maximum absorption wavelength of **CM1** appeared at 390 nm, which was attributed to the π - π^* transition (Figure 3A). Similarly, fluorescence investigation of chemosensor **CM1** was also carried out. When the chemosensor was excited at 390 nm, it gave an emission spectrum of low intensity at 610 nm, which could be attributed to the delocalization of oxygen lone pair electrons towards the aromatic ring, thus causing the quenching of fluorescence via the photoinduced electron transfer (PET) phenomenon (Figure 3B). The IR spectrum of the chemosensor **CM1** is depicted in (Figure S1). The IR spectrum gave the characteristic carbonyl (C=O) peak at 1710 cm^{-1} , while the appearance of peaks at 1628 – 1646 cm^{-1} and 3000 – 2960 cm^{-1} , respectively, corresponded to a C=C aromatic and C-H stretching.

2.2. UV-Visible and Fluorescence Study

The selective chemosensing ability of **CM1** towards Cd^{2+} was investigated through a detailed optical study. The UV-Vis absorption spectra of the **CM1** and **CM1**- Cd^{2+} complex are shown in (Figure 1). The chemosensor **CM1** gave maximum absorbance at 390 nm due to π - π^* transition. Upon the addition of Cd^{2+} , enhancement was observed at the absorption intensity at 390 nm. Similarly, the **CM1** fluorescence spectrum and its response to various metal ions was monitored through its excitation at a maximum wavelength (390 nm) in the aqueous medium. The addition of **CM1** to metal ions, such as Cd^{2+} , Mn^{2+} , Cu^{2+} , Co^{2+} , Ce^{3+} , K^+ , Hg^{2+} , and Zn^{2+} , showed very low enhancement in the fluorescence intensity, but maximum enhancement was observed for Cd^{2+} (Figure 2). This enhancement in fluorescence intensity was probably due to large rigidity in conjugation and better coplanarity upon complexation with the Cd^{2+} ion. In the case of other metal ions, the same phenomenon could not take place, thus inhibiting a significant enhancement in fluorescence intensity [29–31]. Potassium (K) and cerium (Ce) also showed a low fluorescence enhancement, and it may be possible that factors beyond the MLCT and LMCT effects, such as the shape and size of the metal ion, and its ability to accommodate the ligand, could be contributing to this similarity.

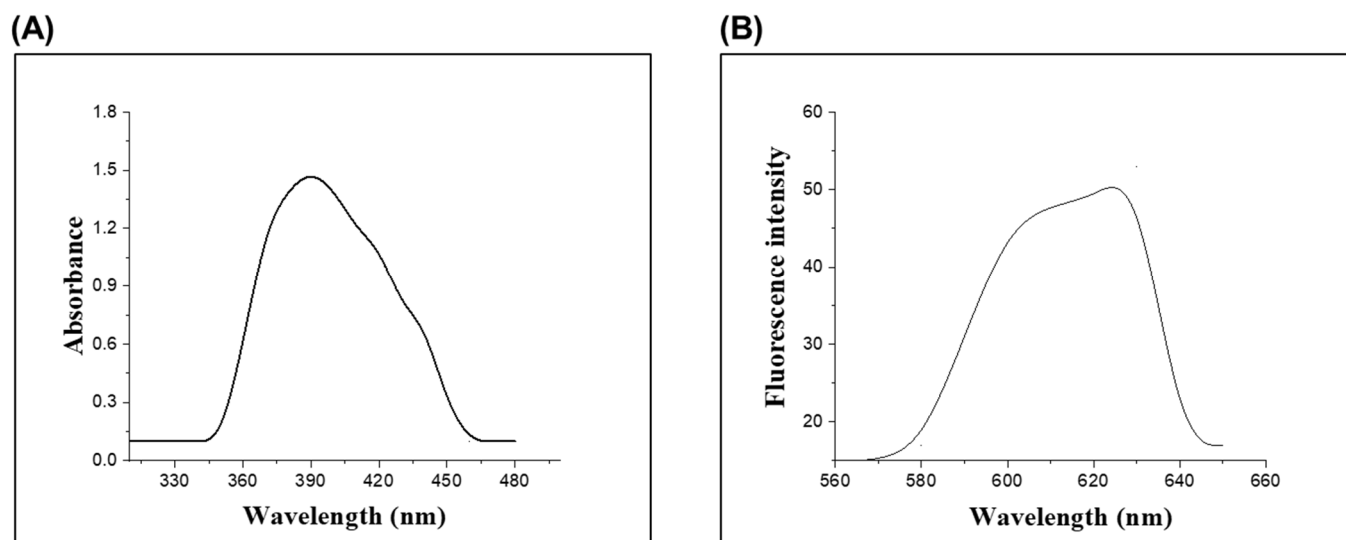


Figure 1. Absorption study of CM1 (10 μM) and CM1 complex with Cd²⁺ (18 μM).

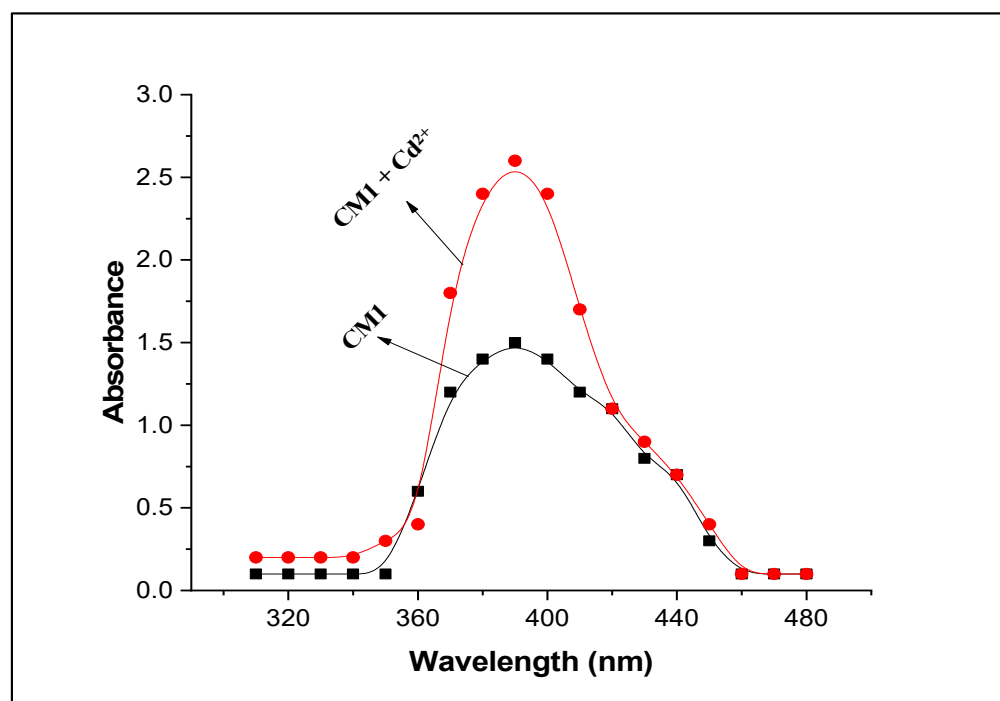


Figure 2. Initial fluorescence study CM1 (10 μM) and metal ions (200 μM), at $\lambda_{ex} = 390$ nm and $\lambda_{em} = 610$ nm.

2.3. Stokes Shift

The reason for the observed large Stokes shifts was intra-molecular charge-transfer excitation of an electron from the HOMO to the LUMO of the chromophore, accompanied by elongation of the bond and considerable solvent reorganization due to hydrogen bonding to the solvent. The chemosensor CM1 showed a prominent Stokes shift, and it can be used for practical application for the detection of Cd²⁺ [32].

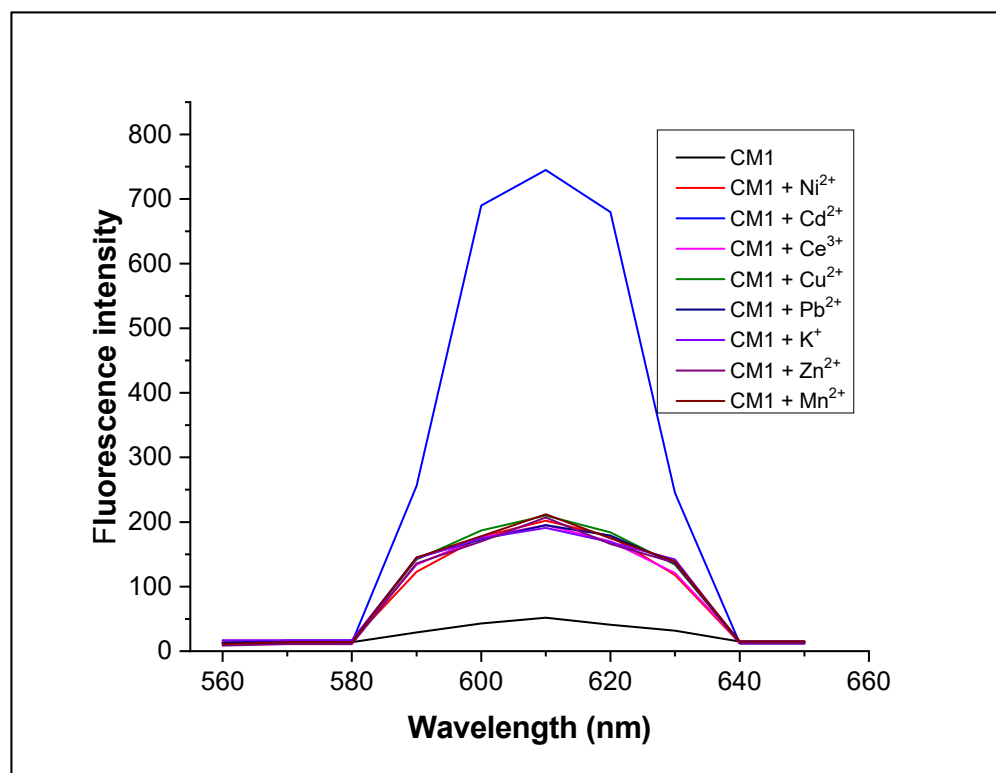
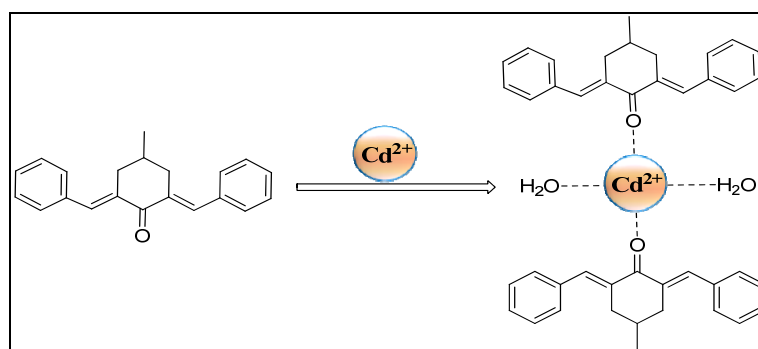


Figure 3. (A) UV-Visible absorption spectrum of chemosensor **CM1**. (B) Fluorescence emission spectrum of the chemosensor **CM1** when excited at 390 nm.

2.4. Detection Limit and Quantum Yield

The LOD for the current chemosensor **CM1** was calculated to be 19.25 nM, as shown in Figure 5 [33]. The predictable mechanism of complex formation is given in Scheme 1.



Scheme 1. With a Cd^{2+} ion.

The quantum yield calculated using Equation (2) for the current chemosensor **CM1** for Cd^{2+} detection was found to be 74%. Rhodamin 6G was chosen as the standard for quantum yield calculation because it is readily available and easily dissolvable in acetonitrile. Additionally, Rhodamine 6G has previously served as a standard for fluorescent chemosensors over a wide range of 340–540 [34].

2.5. Reuseability Study

The reuseability of the chemosensor **CM1** in the detection of Cd^{2+} ion is important for its practical applications. To check the reuseability of chemosensor **CM1**, a reversibility test was carried out using EDTA as chelating agent in aqueous medium at room temperature. The **CM1** can be freed and regenerated by the addition of EDTA to the Cd^{2+} -**CM1** complex

solution, which was observed through diminished fluorescence intensity. The enhanced fluorescence intensity was resumed by the addition of Cd^{2+} solution, which again combined with the **CM1** chemosensor. These results are a reflection of **CM1** as a reusable chemosensor in the presence of an EDTA solution (Figure 4). The results indicated that the same chemosensor, **CM1**, could be used for Cd^{2+} detection up to five times, with consistent and satisfactory outcomes.

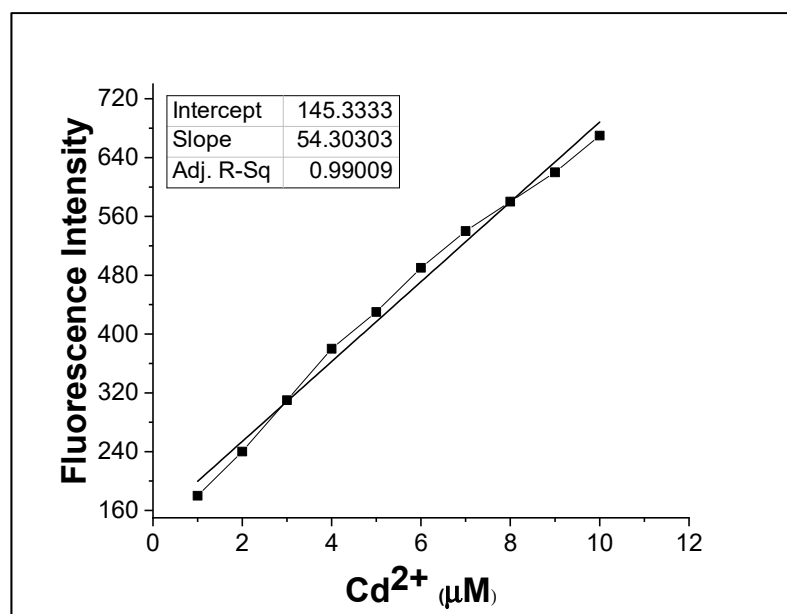


Figure 4. Reusability study of **CM1** (10 μM) with Cd^{2+} (18 μM) and EDTA (18 μM).

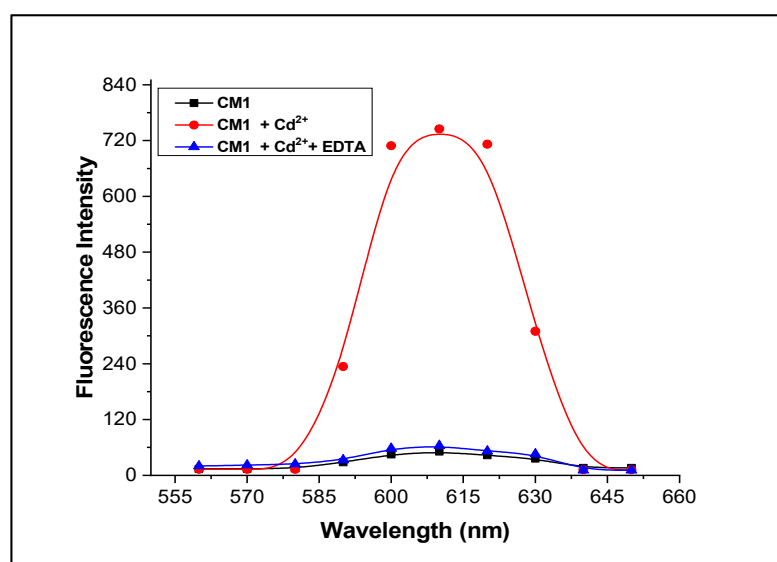


Figure 5. Calibration curve from fluorescence titration of Cd^{2+} (1–10 μM) range and **CM1** (10 μM) at $\lambda_{\text{ex}} = 390 \text{ nm}$ and $\lambda_{\text{em}} = 610 \text{ nm}$.

2.6. Effect of pH

The dependence of pH variation on the fluorescence intensity of free **CM1** and its Cd^{2+} complex was investigated in the pH range of 2.0–12.0 (Figure 6). The pH of the test solution was adjusted with the help of a universal buffer. In case of a free chemosensor, fluorescence intensity remained constant from 2–12 pH, with weak fluorescence intensity. The low fluorescence intensity of **CM1** could be due to the photoinduced electron transfer

(PET) phenomenon. However, for the Cd^{2+} ($18 \mu\text{M}$) complex with **CM1**, the fluorescence intensity gradually increased with pH. Comparatively low fluorescence intensity of the Cd^{2+} complex at lower pH was observed due to the protonation of carbonyl oxygen, which blocked the complexing ability of **CM1**. The maximum fluorescence intensity for the Cd^{2+} complex was obtained at pH 7 due to the restriction of PET. The fluorescence intensity decreased again with pH increase beyond 8 due to possible formation of sparingly soluble hydroxides complex. These results indicate that chemosensor **CM1** can be efficiently employed for Cd^{2+} detection at pH 7 [28].

The decreased fluorescence of the mixture of ligand and Cd^{2+} at both pH 3 and pH 12, as well as the lower fluorescence of the free ligand in the presence of excess cadmium, may be attributed to the formation of a non-fluorescent complex between the ligand and the metal ion. This complex may possess different structural and electronic properties compared to the free ligand, leading to a reduction in its fluorescence intensity. Additionally, factors, such as quenching, energy transfer, or changes in the solvent environment, may also play a role in the observed decrease in fluorescence. The decreased fluorescence of the mixture of ligand and Cd^{2+} at both pH 3 and pH 12, as well as the lower fluorescence of the free ligand in the presence of excess cadmium, may be attributed to the formation of a non-fluorescent complex between the ligand and the metal ion. This complex may possess different structural and electronic properties compared to the free ligand, leading to a reduction in its fluorescence intensity. Additionally, factors, such as quenching, energy transfer, or changes in the solvent environment, may also play a role in the observed decrease in fluorescence.

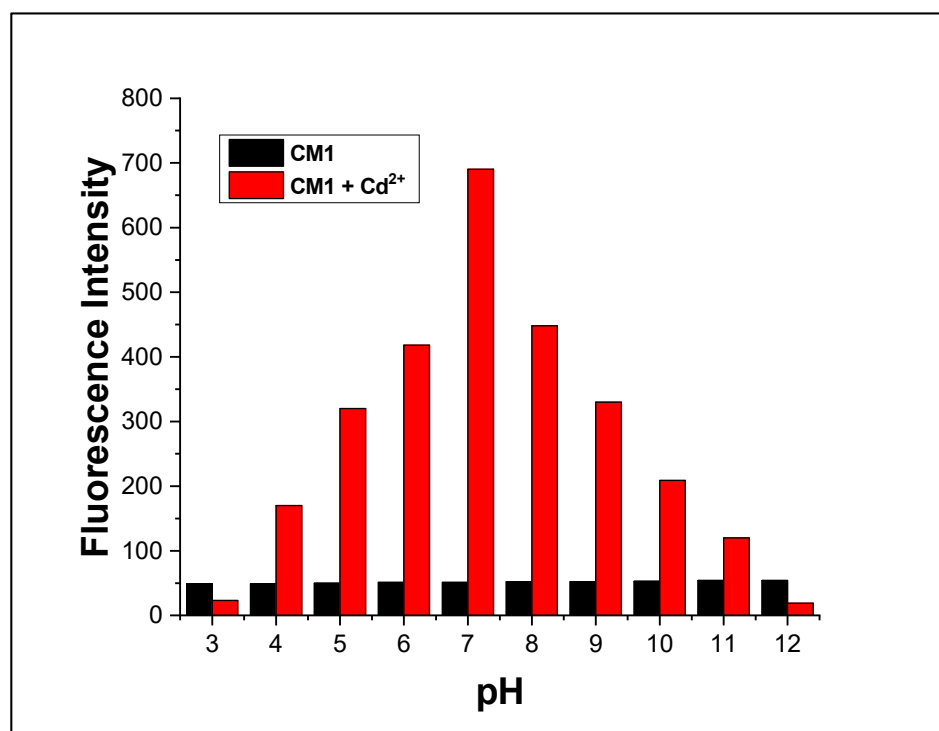


Figure 6. Effect of pH on fluorescence intensity of **CM1** and **CM1** ($10 \mu\text{M}$) with Cd^{2+} ($18 \mu\text{M}$) at $\lambda_{\text{ex}} = 390 \text{ nm}$ and $\lambda_{\text{em}} = 610 \text{ nm}$.

2.7. Anti-Interference Studies

Anti-interference or competitive studies were carried out to verify the selectivity and specificity of the **CM1** for Cd^{2+} in the presence of other metal cations, such as Mn^{2+} , Cu^{2+} , Co^{2+} , Ce^{3+} , K^+ , Hg^{2+} , and Zn^{2+} . The results (Figure 7) showed that these interfering metal ions do not affect the fluorescence intensity of chemosensor **CM1**- Cd^{2+} complex even in the presence of higher concentration of interfering ions. Thus, this indicated that chemosensor

CM1 can be useful as a highly selective fluorescence-on sensor for trace determination of Cd^{2+} ions in different water samples [35–37].

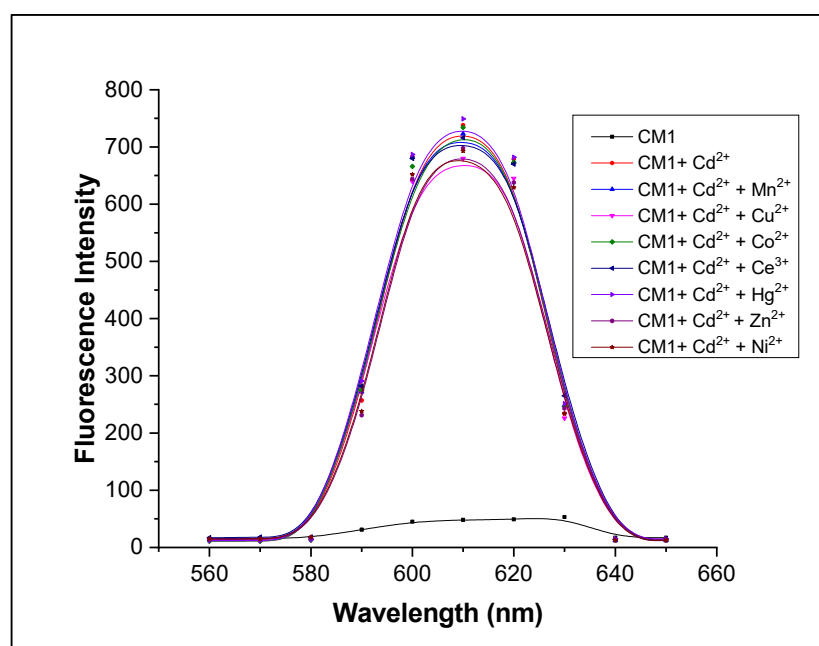


Figure 7. Interference study of **CM1** (10 μM) and Cd^{2+} (18 μM) and interfering metal ions (200 μM) at $\lambda_{\text{ex}} = 390 \text{ nm}$ and $\lambda_{\text{em}} = 610 \text{ nm}$.

2.8. Natural Water Samples Analysis by Spiking

Chemosensor **CM1** was applied for the selective detection of Cd^{2+} in lake water, tap water, and river water. Because, in these water samples, no Cd^{2+} was present, therefore a cadmium (2–10 μM) concentration range was added, and its fluorescence intensity was recorded at optimized parameters. From the calibration curve, respective Cd^{2+} concentrations were determined, and then % recovery was calculated. The results are shown in Table 1. Accordingly, these results demonstrated an excellent recovery of Cd^{2+} from these studied water samples. Thus, here we present a highly sensitive, selective, and cost-effective method for determination of Cd^{2+} in an aqueous medium with good % recovery [38].

Table 1. Natural water samples spiking analysis using **CM1** (10 μM) and Cd^{2+} ion (2–10 μM) range.

Type of Water Sample	Amount of Cd^{2+} Added (μM)	Amount of Cd^{2+} Found (μM)	% Recovery
Tap water	2	2.7	94
	4	4.6	96
	6	5.4	96
	8	7.5	97
	10	9.6	96
River water	2	4.8	95
	4	2.6	96
	6	4.5	97
	8	7.4	97
	10	9.4	96
Lake water	2	2.6	95
	4	3.4	95
	6	5.3	96
	8	7.6	97
	10	9.3	97

2.9. DFT Studies

The detection of Cd^{2+} with the help of chemosensor **CM1** was validated through computational investigation concerning the stability, orbital overlapping of Cd^{2+} and **CM1**, bond angles, bond lengths, and optimized geometry of the resulting cadmium complex. The optimized geometry of the **CM1** and its cadmium complex are shown in Figure 8. The **CM1** acted as a monodentate ligand attached through an oxygen atom to the Cd^{2+} ion, forming a stable distorted tetrahedral geometry.

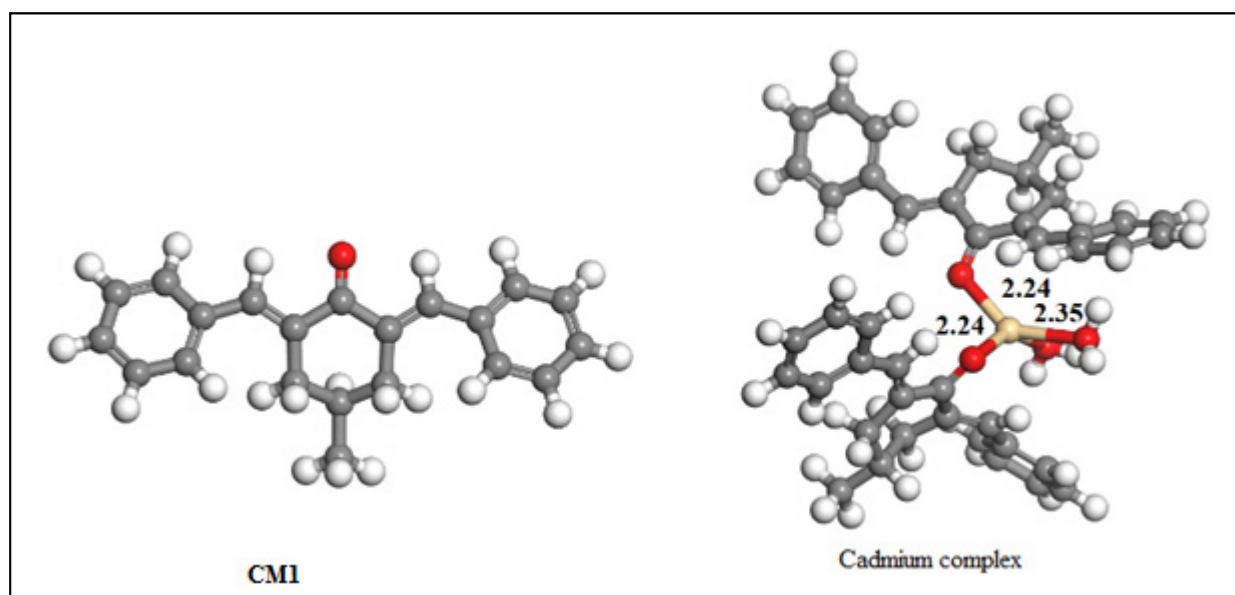


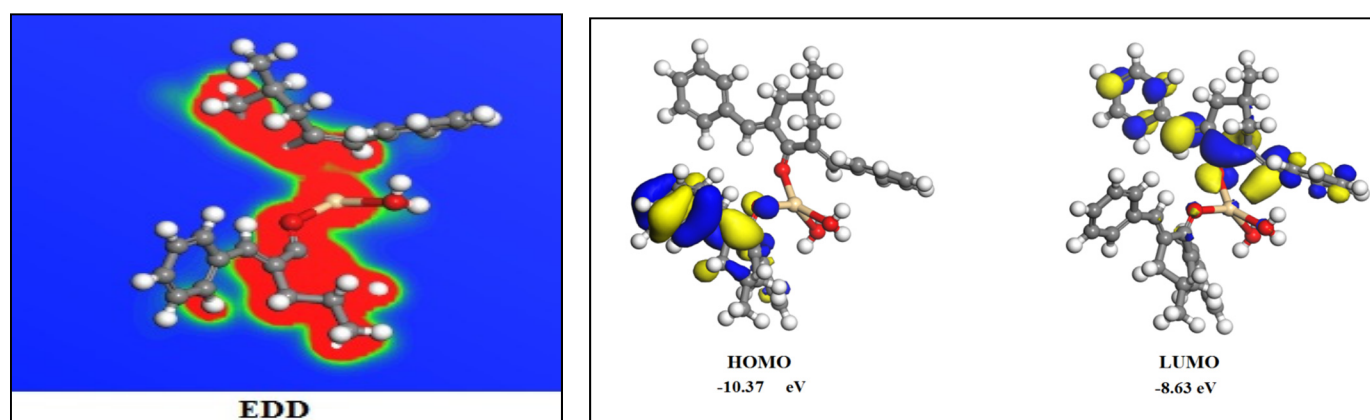
Figure 8. Optimized geometry of the chemosensor **CM1** and its cadmium complex.

The observed bond length, bond angles, metal–ligand interaction energy, charges on oxygen and cadmium, and highest occupied molecular orbital (HOMO) and lowest unoccupied molecular orbital (LUMO) energies of the cadmium complex are listed in Table 2. The observed Cd–O bond lengths with **CM1** were 2.24 Å and Cd–O bond lengths with a water value of 2.35 Å. The shorter Cd–O bond lengths with **CM1**, as compared to water oxygen, was due to the extensive delocalization of electrons on chemosensor **CM1** aromatic rings that made their donor oxygen atom more electron-rich and, hence, caused strong interaction with an electron-deficient metal center. The observed $\text{O}_{\text{CM-1}}\text{-Cd-O}_{\text{CM-1}}$ and $\text{O}_{\text{CM-1}}\text{-Cd-O}_{\text{water}}$ bond angles were 103.08 and 99.24°, respectively, suggesting a distorted tetrahedral complex. The tetrahedral geometry of the complex could also be explained based on orbital hybridization and their involvement in bond formation, since, in Cd^{2+} , all the d orbitals are filled (d^{10} system). Therefore, no orbital in the “d” subshell was available for overlapping with chemosensor **CM1** filled orbital. Hence, the outer s and p subshells underwent sp^3 hybridization and, consequently, formed tetrahedral structures. However, the small deviation from the regular tetrahedral structure was due to the bulky nature of the chemosensor **CM1**. The stability of the resulting Cd^{2+} complex was computationally calculated to be -14.35 eV, and the negative sign indicated the thermodynamic stability of the complex. It is worth noting that MLCT and LMCT effects, while useful for explaining metal–ligand interactions, are not the only contributing factors. Factors, such as the electronic configuration of the metal ion and the ligand, steric effects, and solvent effects, can also play a role in complexation.

Table 2. Binding energies of CM1 and its Cd²⁺ complex.

Bond Length	Bond Angles	Metal CM1 Interaction Energy	HOMO Energy	LUMO Energy	Band Gap	Charges on CM1	Charges after Complexation
2.35 Å (Cd-O _{water})	103.08° (O _{CM-1} -Cd-O _{CM-1})	-14.3559 eV	-10.37eV	-8.63 eV	1.74	O _{water} = -0.309 O _{CM-1} = -0.235	O _{water} = -0.208 O _{CM-1} = -0.215 Cd = 0.6352
2.24 Å Cd-O _{CM-1}	99.24° (O _{CM-1} -Cd-O _{water})						

The interaction between Cd²⁺ and chemosensor **CM1** in the synthesized cadmium complex was also verified from the electron density difference (EDD) analysis. The EDD contour map shown in (Figure 9) indicated the concentration of a large electron cloud along the cadmium–chemosensor **CM1** axis. The HOMO and LUMO band gap gave information about the charge transfer interaction in a molecule. The electron transfer was efficient from the HOMO to LUMO, as the energy gap between these two orbitals became small. The negative value of HOMO and LUMO orbitals depicted in (Table 2) indicated the thermodynamic stability of the complex. The HOMO contained mostly the electron clouds on chemosensor **CM1**, while the Cd²⁺ ion contained a small electron density in LUMO, suggesting the transfer of an electron from chemosensor **CM1** to the cadmium ion upon complex formation. The smaller band gap (1.74) value suggested the utilization of the complex in semiconductor materials [39]. The formation of the cadmium complex was also supported by the extent of electron density transfer from both the oxygen atom of chemosensor **CM1** and water attached to Cd²⁺. As is obvious from Table 2, the formation of the complex caused a reduction in the electron density on the donor atoms of **CM1**, suggesting the formation of the complex. The absorption and fluorescence analysis showed that almost every metal atom was capable of forming a complex with the ligand. However, the highest enhancement was observed in the case of cadmium, indicating a high selectivity for this particular metal ion. Thus, we proceeded to investigate only the complexation reaction between the ligand and cadmium through DFT calculations. Our experimental results were supported by the DFT calculations, which confirmed the stability of the complex.

**Figure 9.** EDD map and the HOMO–LUMO orbitals of the cadmium complex.

2.10. Comparison with REPORTED Chemosensors

The sensitivity of **CM1** was compared with previously reported chemosensors for the determination of Cd²⁺ ions. The result demonstrated that chemosensor **CM1** showed excellent sensitivity, as compared to the reported chemosensors (Table 3). The literature study also showed the lower limit of detection for chemosensor **CM1**, as compared to most of the recently reported similar work, indicating its superiority in terms of selectivity and practical applicability.

Table 3. Comparison of sensitivity (LOD) of **CM1** with other reported chemosensors.

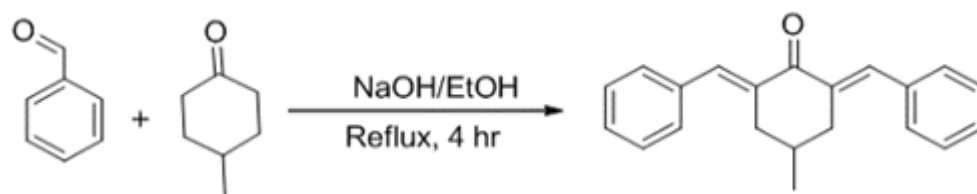
Chemosensors	Analytes	LOD (nM)	pH	Detection Matrixes	References
5-(4-Aminophenyl)-10,15,20-triphenylporphyrin	Cd ²⁺	73	6–8.5	Aqueous media	[40]
Conjugated Polydiacetylenes	Cd ²⁺	185	7.4	Aqueous media	[41]
(<i>E</i>)-4-hydroxy-3-(3-(4-methoxyphenyl)acryloyl)-2 <i>H</i> -chromen-2-one	Cd ²⁺	58.4	7.0	Mixed aqueous–organic media	[28]
4-((pyridin-2-ylmethyl)carbamoyl)phenyl pentacosanoate	Cd ²⁺	2000	NA	Aqueous media	[42]
Bis((indol-3-yl)methylene)oxalohydrazonamide	Hg ²⁺ , Cu ²⁺ , Cd ²⁺	110	NA	Aqueous media	[43]
ZnS quantum dots	Cd ²⁺	37.8	5.6 to 11.5	Aqueous media	[44]
Zn-based azine-functionalized TMU-16 MOF	Cd ²⁺ , Fe ³⁺	500	NA	Aqueous media	[45]
aptasensor	Cd ²⁺	340	7.0	Aqueous media	[46]
AIE fluorescent probe	Cd ²⁺	500	8.0	Aqueous media	[47]
2,6-di((<i>E</i>)-benzylidene)-4-methylcyclohexan-1-one	Cd ²⁺	19.25	7.0	Aqueous media	Present work

3. Materials and Methods

The chemicals and solvents used in the present study were analytical grade and utilized without further purification; the water employed in the experiment was double distilled. The metal salts of NiSO₄·6H₂O, Ca(OH)₂·4H₂O, Mn(OH)₂·4H₂O, ZnSO₄·6H₂O, Cd(SO₄)₂·3H₂O, Cu(SO₄)₂·5H₂O, Co(OH)₃·6H₂O, CrCl₃·6H₂O, KNO₃, Hg(NO₃)₂, Pb(NO₃)₂, and Ce(NO₃)₃·6H₂O were purchased from BDH chemical, England. As Ca(OH)₂ was easily available in our laboratory, we utilized it as a source of calcium. Similarly, nitrate and sulphate salts of other metals were used. Sodium hydroxide, 4-methyl cyclohexanone, benzaldehyde, methanol, and acetonitrile were purchased from Sigma Aldrich and Merck. The UV-Visible spectra were obtained using a double-beam UV/VIS spectrophotometer (Shimadzu, Japan) model 1601. The fluorescent measurement was obtained through spectrophotofluorometer model no RF5301 PC (Shimadzu, Japan), containing a Xenon lamp as a source of excitation. The infra-red spectra were obtained through FT-IR spectrophotometer model 1601 (Shimadzu, Japan). The ¹H NMR spectra were obtained on Prestige 21 (Shimadzu, Japan) using a Bruker Advance 400 MHz spectrometer. The spectrum was obtained in CDCl₃ solution using tetramethyl silane (TMS) as an internal standard.

3.1. Synthesis of Chemosensor **CM1**

The chemosensor **CM1** [(2,6-di((*E*)-benzylidene)-4-methylcyclohexan-1-one)] was synthesized as shown in (Scheme 2) [48–50]. Ethanolic solution of benzaldehyde (1.06 g, 10 mmole) and 4-methyl cyclohexanone (0.49 g, 5 mmole) were mixed with continuous addition of sodium hydroxide (40%). The resulting mixture was refluxed for 4 h. The mixture was cooled to room temperature and evaporated to afford the desired product, **CM1**, as a yellow-colored solid. The crude products were purified by recrystallization from ethanol. Melting point (M. P): 159 °C. Yield: 78%. IR (KBr, cm⁻¹): 1710 cm⁻¹ (C=O stretching), 1628–1646 cm⁻¹ (C=C stretching), 3000–2960 cm⁻¹ (C-H stretching) [51], ¹H-NMR (300 MHz, ppm): δ 7.82 (bs, 2H, CH=C₆H₅), 7.34–7.50 (m, 10H, ArH), 3.07 (dd, *J*_{AB} = 15.9, *J* = 3.6 Hz, 2H, CH₂), 2.53 (m, 2H, 2CH₂), 1.89 (m, 1H, CH), 1.08 (d, 3H *J* = 6.6 Hz, 3H, CHCH₃) [52].



Scheme 2. Synthetic route of chemosensor **CM1**.

3.2. Solutions Preparation for Spectroscopic Measurements

Stock solution of chemosensor **CM1** in acetonitrile, and metal solutions using respective salts were prepared in distilled water. Stock solutions of metal (0.1 mM) were prepared in 100 mL solvent/water. Then working solutions were prepared by taking 5 mL from this stock metal solution and diluting it to 100 mL. Each time, a fresh working solutions of both chemosensor **CM1** and metal ion was prepared.

3.3. General UV–Vis and Fluorescence Spectra Measurements

A stock solution of **CM1** (4 mM) was prepared in acetonitrile. Similarly, the same concentration solutions of the corresponding salts of copper, cerium, cadmium, zinc, mercury, cobalt, and manganese were prepared in double-distilled water. The tested solutions were prepared by mixing 50 μ L stock solution of **CM1** with the appropriate amount of each metal ion in a tube. Absorption spectra were taken from the 250–500 nm range. Based on UV-Vis analysis, the fluorescent measurements were set at 390 nm. Each spectrum was taken three times, and their mean value was considered as final data. The chemosensing utility of **CM1** for Cd^{2+} in the presence of other metal ions was also investigated in natural water samples.

3.4. Excitation and Emission Spectra of Chemosensor **CM1**

Upon exciting chemosensor **CM1** at $\lambda_{\text{exc}} = 390$ nm, its fluorescence emission spectrum was recorded in the range of 230–800 nm. A weak fluorescence emission spectrum was observed at $\lambda_{\text{em}} = 610$ nm. Thus, at these wavelengths of excitation and emission, further fluorometric analyses were carried out.

3.5. Limit of Detection and Quantum Yield Calculation

The limit of detection (LOD) was calculated to be 19.25 nM from the calibration curve using Equation (1).

$$\text{LOD} = \frac{3\delta}{S} \quad (1)$$

In Equation (1) “ δ ” represents the standard deviation, and “ S ” is the slope of the fluorescence intensity vs. sample concentration curve.

Rhodamine 6G dye was used as a standard possessing a quantum yield (φ) 95 % for enumerating the quantum yield of the chemosensor **CM1** because Rhodamine 6G dye is readily available and easily dissolvable in acetonitrile. Additionally, Rhodamine 6G can be used as a standard for fluorescent chemosensors over a wide range of 340–540 [34,53]. For the experiment, Rhodamine 6G solution was prepared, and its spectroscopic analysis (UV-visible and fluorescence) were performed. The quantum yield was determined with the help of Equation (2).

$$\varphi_{\text{C}} = \varphi_{\text{R}} \left(\frac{I_{\text{C}}}{I_{\text{R}}} \right) \left(\frac{\eta_{\text{C}}^2}{\eta_{\text{R}}^2} \right) \left(\frac{A_{\text{R}}}{A_{\text{C}}} \right) \quad (2)$$

where “ C ” and “ R ” represent chemosensor **CM1** and dye, respectively. “ I ” represents the integrated fluorescence intensity, “ η ” corresponds to the refractive index of the solvent, and “ A ” corresponds to absorbance.

The values of absorbance in the equation were determined and used. For Equation (2), $\varphi_{\text{R}} = 0.95$, $I_{\text{R}} = 620$, $\eta_{\text{R}} = 1.33$, $A_{\text{R}} = 0.209$, $I_{\text{C}} = 40$, $\eta_{\text{C}} = 1.34$, and $A_{\text{C}} = 1.5$.

3.6. Spiked Water Samples Analysis

Natural water samples were collected from River Swat at Chakdara point, Malakand Lake at Dargai, and from the University of Malakand campus, respectively. Since no cadmium was found in these samples, the applicability of the new chemosensor **CM1** was determined by the spiking technique. A known amount of Cd^{2+} was added to each water sample, and the fluorescence intensity of spiked water samples was recorded. The selected water samples were spiked with different concentrations of Cd^{2+} (5–10) μM in the presence of chemosensor **CM1** (10 μM). The fluorescence response was measured at specific wavelengths of excitation and emission. For verification of the test results, each spectral analysis was carried out three times.

3.7. Theoretical Calculation

The density functional theory (DFT) calculations were employed utilizing DMol3 simulation code [54,55]. The geometry and energy of the synthesized chemosensor **CM1** were optimized through Perdew Burke Ernzerhoffunctional (PBE) in the domain of generalized gradient approximation (GGA) [56,57]. The double numerical plus polarization (DNP) (Liu and Rodriguez 2005) was used for the adjustment of the basis set for all types of computation. Hessian calculations showed the absence of any imaginary frequency that reflects the stability of the relaxed structure. The thermal smearing parameters and basis set cut-off were adjusted, respectively, to 0.005 au and 4.6 Å. Grimme's scheme DFT-D2 empirical dispersion correction was employed for van der Waals intermolecular interactions [58,59]. Convergence tolerance of 10^{-5} Ha for energy, 0.001 H/Å for force, and 0.005 Å for displacement were set during the geometries' relaxation. The adsorption energies (E_{int}) of complexes were evaluated using the following equation.

$$E_{\text{int}} = E_{\text{complex}} - (E_{\text{CM1}} + E_{\text{Cd(II)}}) \quad (3)$$

where, E_{complex} , E_{lignd} , and $E_{\text{Cd(II)}}$ are the total-electronic energies of the Cd(II)-**CM1** (complex), **CM1** and Cd(II) ion), respectively.

4. Conclusions

In summary, we have presented, here, the design and development of a novel optical chemosensor based on a curcumin derivative *CMI*, which can detect Cd^{2+} over other competitive metal ions in an aqueous medium. *CMI* exhibited good photostability and enhanced fluorescence in an aqueous medium upon the formation of the Cd^{2+} complex due to the presence of a carbonyl oxygen group. The interaction ratio between chemosensor *CMI* and Cd^{2+} ion was determined by fluorescence titration, Job's plot, and computational studies, and it was found to be 2:1. The competitive binding experiment revealed no interference from the other metal ions (Mn^{2+} , Ni^{2+} , Cu^{2+} , Co^{2+} , Ce^{3+} , K^{+} , Hg^{2+} , and Zn^{2+}), thus showing selectivity of **CM1** towards Cd^{2+} . Moreover, **CM1** showed high sensitivity at physiological pH, with low detection limits (19.25 nM). The **CM1**-based chemosensor can be recycled and reused multiple times with the addition of an EDTA solution. This sensing approach certainly provides a basis that can be used for the design of various curcumin-based optical chemosensors to monitor other environmentally concerned hazardous heavy metal ions in aqueous medium.

Supplementary Materials: The following supporting information can be downloaded at: <https://www.mdpi.com/article/10.3390/molecules28083635/s1>, Figure S1 [60,61]: FT-IR spectrum of chemosensor **CM1**; Figure S2: $^1\text{H-NMR}$ spectrum of the chemosensor **CM1**; Figure S3: Job's plot analysis of **CM1** shows 2:1 binding ratio between chemosensor **CM1** and Cd^{2+} .

Author Contributions: Conceptualization, M.S. and J.K.; methodology, R.K. and J.K.; validation, M.Z., M.S., A.W.K., A.B., E.A.A. and R.U.; formal analysis, A.W.K. and A.B.; investigation, A.B. and R.U.; data curation, J.K. and M.S.; writing—original draft preparation J.K., M.Z., M.S. and R.K.;

writing—review and editing, M.Z., R.U., R.K., E.A.A. and A.B. All authors have read and agreed to the published version of the manuscript.

Funding: The research work was supported by researchers supporting project number (RSP2023R45) at King Saud University, Riyadh, Saudi Arabia.

Institutional Review Board Statement: Not applicable.

Informed Consent Statement: Not applicable.

Data Availability Statement: Not applicable.

Acknowledgments: The authors extend their appreciation to the researchers supporting Project number (RSP2023R45) King Saud University, Riyadh, Saudi Arabia, for financial support.

Conflicts of Interest: The authors declare no conflict of interest.

Sample Availability: Samples of the compounds are available from the authors.

References

1. Wang, J.; Xia, T.; Zhang, X.; Zhang, Q.; Cui, Y.; Yang, Y.; Qian, G. A Turn-on Fluorescent Probe for Cd²⁺ Detection in Aqueous Environments Based on an Imine Functionalized Nanoscale Metal–Organic Framework. *RSC Adv.* **2017**, *7*, 54892–54897. [[CrossRef](#)]
2. El-Saadani, Z.; Mingqi, W.; He, Z.; Hamukwaya, S.L.; Abdel Wahed, M.S.M.; Abu Khatita, A. Environmental Geochemistry and Fractionation of Cadmium Metal in Surficial Bottom Sediments and Water of the Nile River, Egypt. *Toxics* **2022**, *10*, 221. [[CrossRef](#)]
3. Barone, G.; Storelli, A.; Garofalo, R.; Mallamaci, R.; Storelli, M.M. Residual Levels of Mercury, Cadmium, Lead and Arsenic in Some Commercially Key Species from Italian Coasts (Adriatic Sea): Focus on Human Health. *Toxics* **2022**, *10*, 223. [[CrossRef](#)]
4. Smichowski, P.; Londonio, A. The Role of Analytical Techniques in the Determination of Metals and Metalloids in Dietary Supplements: A Review. *Microchem. J.* **2018**, *136*, 113–120. [[CrossRef](#)]
5. He, D.; Zhu, Z.; Miao, X.; Zheng, H.; Li, X.; Belshaw, N.S.; Hu, S. Determination of Trace Cadmium in Geological Samples by Membrane Desolvation Inductively Coupled Plasma Mass Spectrometry. *Microchem. J.* **2019**, *148*, 561–567. [[CrossRef](#)]
6. Haribala; Hu, B.; Wang, C.; Gerilemandahu; Xu, X.; Zhang, S.; Bao, S.; Li, Y. Assessment of Radioactive Materials and Heavy Metals in the Surface Soil around Uranium Mining Area of Tongliao, China. *Ecotoxicol. Env. Saf.* **2016**, *130*, 185–192. [[CrossRef](#)]
7. Lee, W.; Kim, H.; Kang, Y.; Lee, Y.; Yoon, Y. A Biosensor Platform for Metal Detection Based on Enhanced Green Fluorescent Protein. *Sensors* **2019**, *19*, E1846. [[CrossRef](#)]
8. Yao, Y.; Wu, H.; Ping, J. Simultaneous Determination of Cd(II) and Pb(II) Ions in Honey and Milk Samples Using a Single-Walled Carbon Nanohorns Modified Screen-Printed Electrochemical Sensor. *Food Chem.* **2019**, *274*, 8–15. [[CrossRef](#)]
9. Lin, L.; Wang, Y.; Xiao, Y.; Liu, W. Hydrothermal Synthesis of Carbon Dots Codoped with Nitrogen and Phosphorus as a Turn-on Fluorescent Probe for Cadmium(II). *Microchim. Acta* **2019**, *186*, 147. [[CrossRef](#)]
10. Pan, Y.; Xiao, W.; Fan, M.; Chen, W.; Xu, S. Detection of Cd(II) Ions by a Self-Tuning Method Using Quantum Dot Fluorescence Sensing. *Mater. Res. Express* **2017**, *4*, 105008. [[CrossRef](#)]
11. Petryayeva, E.; Algar, W.R.; Medintz, I.L. Quantum Dots in Bioanalysis: A Review of Applications across Various Platforms for Fluorescence Spectroscopy and Imaging. *Appl. Spectrosc.* **2013**, *67*, 215–252. [[CrossRef](#)]
12. Carter, K.P.; Young, A.M.; Palmer, A.E. Fluorescent Sensors for Measuring Metal Ions in Living Systems. *Chem. Rev.* **2014**, *114*, 4564–4601. [[CrossRef](#)]
13. Li, J.; Yim, D.; Jang, W.-D.; Yoon, J. Recent Progress in the Design and Applications of Fluorescence Probes Containing Crown Ethers. *Chem. Soc. Rev.* **2017**, *46*, 2437–2458. [[CrossRef](#)]
14. Zhu, H.; Fan, J.; Wang, B.; Peng, X. Fluorescent, MRI, and Colorimetric Chemical Sensors for the First-Row d-Block Metal Ions. *Chem. Soc. Rev.* **2015**, *44*, 4337–4366. [[CrossRef](#)]
15. Ding, X.; Zhang, F.; Bai, Y.; Zhao, J.; Chen, X.; Ge, M.; Sun, W. Quinoline-Based Highly Selective and Sensitive Fluorescent Probe Specific for Cd²⁺ Detection in Mixed Aqueous Media. *Tetrahedron Lett.* **2017**, *58*, 3868–3874. [[CrossRef](#)]
16. Kim, H.N.; Ren, W.X.; Kim, J.S.; Yoon, J. Fluorescent and Colorimetric Sensors for Detection of Lead, Cadmium, and Mercury Ions. *Chem. Soc. Rev.* **2012**, *41*, 3210–3244. [[CrossRef](#)]
17. Qian, J.; Wang, K.; Wang, C.; Ren, C.; Liu, Q.; Hao, N.; Wang, K. Ratiometric Fluorescence Nanosensor for Selective and Visual Detection of Cadmium Ions Using Quencher Displacement-Induced Fluorescence Recovery of CdTe Quantum Dots-Based Hybrid Probe. *Sens. Actuators B Chem.* **2017**, *241*, 1153–1160. [[CrossRef](#)]
18. Shi, C.; Huang, Z.; Wu, A.; Hu, Y.; Wang, N.; Zhang, Y.; Shu, W.; Yu, W. Recent Progress in Cadmium Fluorescent and Colorimetric Probes. *RSC Adv.* **2021**, *11*, 29632–29660. [[CrossRef](#)]
19. Su, W.; Yuan, S.; Wang, E. A Rhodamine-Based Fluorescent Chemosensor for the Detection of Pb²⁺, Hg²⁺ and Cd²⁺. *J. Fluoresc.* **2017**, *27*, 1871–1875. [[CrossRef](#)]
20. Zhang, Y.; Guo, X.; Zheng, M.; Yang, R.; Yang, H.; Jia, L.; Yang, M. A 4,5-Quinolimide-Based Fluorescent Sensor for the Turn-on Detection of Cd²⁺ with Live-Cell Imaging. *Org. Biomol. Chem.* **2017**, *15*, 2211–2216. [[CrossRef](#)]

21. Liu, Z.; Zhang, C.; He, W.; Yang, Z.; Gao, X.; Guo, Z. A Highly Sensitive Ratiometric Fluorescent Probe for Cd²⁺ Detection in Aqueous Solution and Living Cells. *Chem. Commun.* **2010**, *46*, 6138–6140. [[CrossRef](#)] [[PubMed](#)]
22. Wang, Y.; Hu, X.; Wang, L.; Shang, Z.; Chao, J.; Jin, W. A New Acridine Derivative as a Highly Selective ‘off-on’ Fluorescence Chemosensor for Cd²⁺ in Aqueous Media. *Sens. Actuators B Chem.* **2011**, *156*, 126–131. [[CrossRef](#)]
23. Yang, Y.; Cheng, T.; Zhu, W.; Xu, Y.; Qian, X. Highly Selective and Sensitive Near-Infrared Fluorescent Sensors for Cadmium in Aqueous Solution. *Org. Lett.* **2011**, *13*, 264–267. [[CrossRef](#)] [[PubMed](#)]
24. Jiang, X.-J.; Li, M.; Lu, H.-L.; Xu, L.-H.; Xu, H.; Zang, S.-Q.; Tang, M.-S.; Hou, H.-W.; Mak, T.C.W. A Highly Sensitive C3-Symmetric Schiff-Base Fluorescent Probe for Cd²⁺. *Inorg. Chem.* **2014**, *53*, 12665–12667. [[CrossRef](#)] [[PubMed](#)]
25. Khani, R.; Ghiamati, E.; Boroujerdi, R.; Rezaeifard, A.; Zaryabi, M.H. A New and Highly Selective Turn-on Fluorescent Sensor with Fast Response Time for the Monitoring of Cadmium Ions in Cosmetic, and Health Product Samples. *Spectrochim. Acta Part. A Mol. Biomol. Spectrosc.* **2016**, *163*, 120–126. [[CrossRef](#)]
26. Liu, D.; Qi, J.; Liu, X.; Cui, Z.; Chang, H.; Chen, J.; Yang, G. 4-Amino-1,8-Naphthalimide-Based Fluorescent Cd²⁺ Sensor with High Selectivity against Zn²⁺ and Its Imaging in Living Cells. *Sens. Actuators B Chem.* **2014**, *204*, 655–658. [[CrossRef](#)]
27. Mikata, Y.; Kizu, A.; Konno, H. TQPHEN (N,N,N',N'-Tetrakis(2-Quinolylmethyl)-1,2-Phenylenediamine) Derivatives as Highly Selective Fluorescent Probes for Cd²⁺. *Dalton Trans.* **2014**, *44*, 104–109. [[CrossRef](#)]
28. Shaily; Kumar, A.; Ahmed, N. A Coumarin–Chalcone Hybrid Used as a Selective and Sensitive Colorimetric and Turn-on Fluorometric Sensor for Cd²⁺ Detection. *New J. Chem.* **2017**, *41*, 14746–14753. [[CrossRef](#)]
29. Cai, H.; Zou, J.; Lin, J.; Li, J.; Huang, Y.; Zhang, S.; Yuan, B.; Ma, J. Sodium Hydroxide-Enhanced Acetaminophen Elimination in Heat/Peroxymonosulfate System: Production of Singlet Oxygen and Hydroxyl Radical. *Chem. Eng. J.* **2022**, *429*, 132438. [[CrossRef](#)]
30. Li, J.; Zou, J.; Zhang, S.; Cai, H.; Huang, Y.; Lin, J.; Li, Q.; Yuan, B.; Ma, J. Sodium Tetraborate Simultaneously Enhances the Degradation of Acetaminophen and Reduces the Formation Potential of Chlorinated By-Products with Heat-Activated Peroxymonosulfate Oxidation. *Water Res.* **2022**, *224*, 119095. [[CrossRef](#)]
31. Huang, Y.; Zou, J.; Lin, J.; Yang, H.; Wang, M.; Li, J.; Cao, W.; Yuan, B.; Ma, J. ABTS as Both Activator and Electron Shuttle to Activate Persulfate for Diclofenac Degradation: Formation and Contributions of ABTS•+, SO4•-, and •OH. *Environ. Sci. Technol.* **2022**. [[CrossRef](#)]
32. Bie, F.; Cao, H.; Yan, P.; Cui, H.; Shi, Y.; Ma, J.; Liu, X.; Han, Y. A Cyanobiphenyl-Based Ratiometric Fluorescent Sensor for Highly Selective and Sensitive Detection of Zn²⁺. *Inorg. Chim. Acta* **2020**, *508*, 119652. [[CrossRef](#)]
33. Shaji, L.K.; Selva Kumar, R.; Jose, J.; Bhaskar, R.; Vetriarasu, V.; Bhat, S.G.; Ashok Kumar, S.K. Selective Chromogenic and Fluorogenic Signalling of Hg²⁺ Ions Using a Benzothiazole-Quinolyl Acrylate Conjugate and Its Applications in the Environmental Water Samples and Living Cells. *J. Photochem. Photobiol. A Chem.* **2023**, *434*, 114220. [[CrossRef](#)]
34. Bhasin, A.K.K.; Chauhan, P.; Chaudhary, S. A Novel Coumarin-Tagged Ditopic Scaffold as a Selectively Sensitive Fluorogenic Receptor of Zinc (II) Ion. *Sens. Actuators B Chem.* **2021**, *330*, 129328. [[CrossRef](#)]
35. Desai, M.L.; Basu, H.; Saha, S.; Singhal, R.K.; Kailasa, S.K. One Pot Synthesis of Fluorescent Gold Nanoclusters from Curcuma Longa Extract for Independent Detection of Cd²⁺, Zn²⁺ and Cu²⁺ Ions with High Sensitivity. *J. Mol. Liq.* **2020**, *304*, 112697. [[CrossRef](#)]
36. Maity, A.; Ghosh, U.; Giri, D.; Mukherjee, D.; Maiti, T.K.; Patra, S.K. A Water-Soluble BODIPY Based ‘OFF/ON’ Fluorescent Probe for the Detection of Cd²⁺ Ions with High Selectivity and Sensitivity. *Dalton Trans.* **2019**, *48*, 2108–2117. [[CrossRef](#)]
37. Wang, P.; Zhou, D.; Chen, B. A Fluorescent Dansyl-Based Peptide Probe for Highly Selective and Sensitive Detect Cd²⁺ Ions and Its Application in Living Cell Imaging. *Spectrochim. Acta A Mol. Biomol. Spectrosc.* **2019**, *207*, 276–283. [[CrossRef](#)]
38. Kumar, R.S.; Kumar, S.K.A.; Vijayakrishna, K.; Sivaramakrishna, A.; Paira, P.; Rao, C.V.S.B.; Sivaraman, N.; Sahoo, S.K. Bipyridine Bisphosphonate-Based Fluorescent Optical Sensor and Optode for Selective Detection of Zn²⁺ Ions and Its Applications. *New J. Chem.* **2018**, *42*, 8494–8502. [[CrossRef](#)]
39. Ismail, B.A.; Nassar, D.A.; Abd El-Wahab, Z.H.; Ali, O.A.M. Synthesis, Characterization, Thermal, DFT Computational Studies and Anticancer Activity of Furfural-Type Schiff Base Complexes. *J. Mol. Struct.* **2021**, *1227*, 129393. [[CrossRef](#)]
40. Lv, Y.; Wu, L.; Shen, W.; Wang, J.; Xuan, G.; Sun, X. A Porphyrin-Based Chemosensor for Colorimetric and Fluorometric Detection of Cadmium(II) with High Selectivity. *J. Porphyr. Phthalocyanines* **2015**, *19*, 769–774. [[CrossRef](#)]
41. Pham, T.C.; Kim, Y.K.; Park, J.B.; Jeon, S.; Ahn, J.; Yim, Y.; Yoon, J.; Lee, S. A Selective Colorimetric and Fluorometric Chemosensor Based on Conjugated Polydiacetylenes for Cadmium Ion Detection. *ChemPhotoChem* **2019**, *3*, 1133–1137. [[CrossRef](#)]
42. Kim, Y.K.; Pham, T.C.; Kim, J.; Bae, C.; Choi, Y.; Jo, M.H.; Lee, S. Polydiacetylenes Containing 2-Picolylamide Chemosensor for Colorimetric Detection of Cadmium Ions. *Bull. Korean Chem. Soc.* **2021**, *42*, 265–269. [[CrossRef](#)]
43. Yadav, N.; Singh, A.K. Colorimetric and Fluorometric Detection of Heavy Metal Ions in Pure Aqueous Medium with Logic Gate Application. *J. Electrochem. Soc.* **2019**, *166*, B644. [[CrossRef](#)]
44. Liu, Y.; Tang, X.; Deng, M.; Zhu, T.; Edman, L.; Wang, J. Hydrophilic AgInZnS Quantum Dots as a Fluorescent Turn-on Probe for Cd²⁺ Detection. *J. Alloys Compd.* **2021**, *864*, 158109. [[CrossRef](#)]
45. Farahani, Y.D.; Safarifard, V. Highly Selective Detection of Fe³⁺, Cd²⁺ and CH₂Cl₂ Based on a Fluorescent Zn-MOF with Azine-Decorated Pores. *J. Solid State Chem.* **2019**, *275*, 131–140. [[CrossRef](#)]

46. Zhou, B.; Yang, X.-Y.; Wang, Y.-S.; Yi, J.-C.; Zeng, Z.; Zhang, H.; Chen, Y.-T.; Hu, X.-J.; Suo, Q.-L. Label-Free Fluorescent Aptasensor of Cd²⁺ Detection Based on the Conformational Switching of Aptamer Probe and SYBR Green I. *Microchem. J.* **2019**, *144*, 377–382. [[CrossRef](#)]
47. Jiang, H.; Chen, L.; Li, Z.; Li, J.; Ma, H.; Ning, L.; Li, N.; Liu, X. A Facile AIE Fluorescent Probe with Large Stokes Shift for the Detection of Cd²⁺ in Real Water Samples and Living Cells. *J. Lumin.* **2022**, *243*, 118672. [[CrossRef](#)]
48. Carmona-Vargas, C.C.; Alves, L.d.C.; Brocksom, T.J.; De Oliveira, K.T. Combining Batch and Continuous Flow Setups in the End-to-End Synthesis of Naturally Occurring Curcuminoids. *React. Chem. Eng.* **2017**, *2*, 366–374. [[CrossRef](#)]
49. Han, J.; Tang, X.; Wang, Y.; Liu, R.; Wang, L.; Ni, L. A Quinoline-Based Fluorescence “on-off-on” Probe for Relay Identification of Cu²⁺ and Cd²⁺ Ions. *Spectrochim. Acta Part A Mol. Biomol. Spectrosc.* **2018**, *205*, 597–602. [[CrossRef](#)]
50. Khan, J.; Sadia, M.; Wadood Ali Shah, S.; Zahoor, M.; Alsharif, K.F.; Al-Joufi, F.A. Development of [(2E,6E)-2,6-Bis(4-(Dimethylamino)Benzylidene)Cyclohexanone] as Fluorescence-on Probe for Hg²⁺ Ion Detection: Computational Aided Experimental Studies. *Arab. J. Chem.* **2022**, *15*, 103710. [[CrossRef](#)]
51. Mohammadi Ziarani, G.; Badieli, A.; Abbasi, A.; Farahani, Z. Cross-Aldol Condensation of Cycloalkanones and Aromatic Aldehydes in the Presence of Nanoporous Silica-Based Sulfonic Acid (SiO₂-Pr-SO₃H) under Solvent Free Conditions. *Chin. J. Chem.* **2009**, *27*, 1537–1542. [[CrossRef](#)]
52. Tamang, N.; Ramamoorthy, G.; Joshi, M.; Choudury, A.R.; Siva Kumar, B.; Golakoti, N.R.; Doble, M. Diarylidencyclopentanone Derivatives as Potent Anti-Inflammatory and Anticancer Agents. *Med. Chem. Res.* **2020**, *29*, 1579–1589. [[CrossRef](#)]
53. Kubin, R.F.; Fletcher, A.N. Fluorescence Quantum Yields of Some Rhodamine Dyes. *J. Lumin.* **1982**, *27*, 455–462. [[CrossRef](#)]
54. Delley, B. An All-electron Numerical Method for Solving the Local Density Functional for Polyatomic Molecules. *J. Chem. Phys.* **1990**, *92*, 508–517. [[CrossRef](#)]
55. Delley, B. From Molecules to Solids with the DMol3 Approach. *J. Chem. Phys.* **2000**, *113*, 7756–7764. [[CrossRef](#)]
56. Perdew, J.P.; Burke, K.; Ernzerhof, M. Generalized Gradient Approximation Made Simple. *Phys. Rev. Lett.* **1996**, *77*, 3865–3868. [[CrossRef](#)]
57. Liu, P.; Rodriguez, J.A. Catalysts for Hydrogen Evolution from the [NiFe] Hydrogenase to the Ni₂P(001) Surface: The Importance of Ensemble Effect. *J. Am. Chem. Soc.* **2005**, *127*, 14871–14878. [[CrossRef](#)]
58. Grimme, S. Accurate Description of van Der Waals Complexes by Density Functional Theory Including Empirical Corrections. *J. Comput. Chem.* **2004**, *25*, 1463–1473. [[CrossRef](#)]
59. Grimme, S. Semiempirical GGA-type density functional constructed with a long-range dispersion correction. *J. Comput. Chem.* **2006**, *27*, 1787–1799. [[CrossRef](#)]
60. Mehta, P.K.; Hwang, G.W.; Park, J.; Lee, K.H. Highly sensitive ratiometric fluorescent detection of indium (III) using fluorescent probe based on phosphoserine as a receptor. *Anal. Chem.* **2018**, *90*, 11256–11264. [[CrossRef](#)]
61. Wu, X.; Niu, Q.; Li, T. A novel urea-based “turn-on” fluorescent sensor for detection of Fe³⁺/F⁻ ions with high selectivity and sensitivity. *Sens. Actuators B Chem.* **2016**, *222*, 714–720. [[CrossRef](#)]

Disclaimer/Publisher’s Note: The statements, opinions and data contained in all publications are solely those of the individual author(s) and contributor(s) and not of MDPI and/or the editor(s). MDPI and/or the editor(s) disclaim responsibility for any injury to people or property resulting from any ideas, methods, instructions or products referred to in the content.